Chandra view on the active nucleus of the restarted radio galaxy CGCG 292-057

K. Balasubramaniam[1] , Ł. Stawarz[1] , V. Marchenko[1] , R. Thimmappa[1] , M. Sobolewska[2] , A. Siemiginowska[2] , C.C. Cheung[3] , D. Kozieł-Wierzbowska[1] & M. Jamrozy[1]

[1]Astronomical observatory, Jagiellonian university, Orla 171, 30-244 Krakow, Poland (email: karthik@oa.uj.edu.pl)

[2]Harvard Smithsonian Center for Astrophysics, 60 Garden St, Cambridge, MA 02138, USA;

[3]Space Science Division, Naval Research Laboratory, Washington, DC 20375-5352, USA)

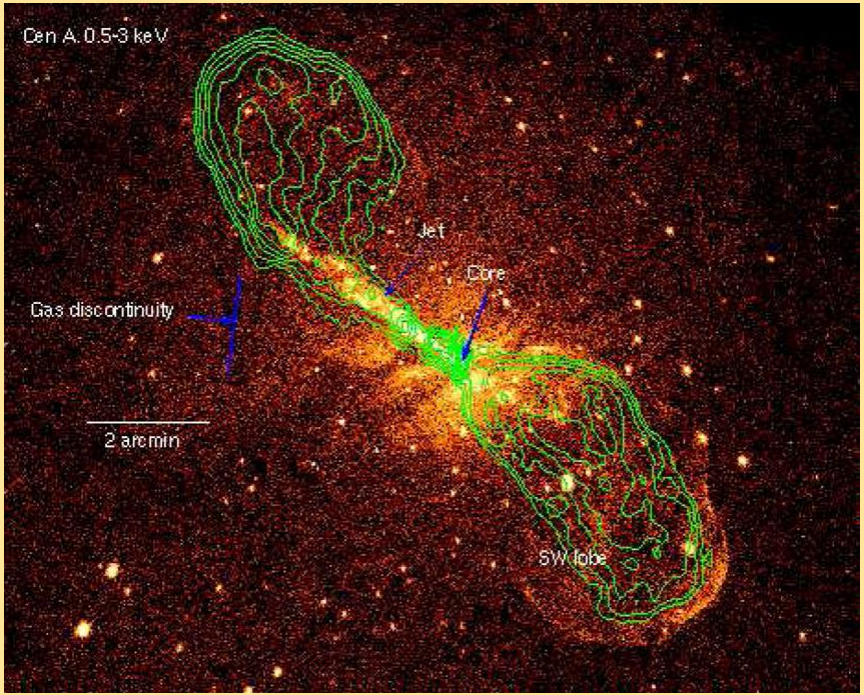

Radio contours on a deep *Chandra* image of Cen A, showing the core and NE jet crossed by absorption stripes corresponding to NGC 5128's dust lanes, the SW lobe, structures associated with the NE lobe, the position of a merger-related gas discontinuity that is shown.

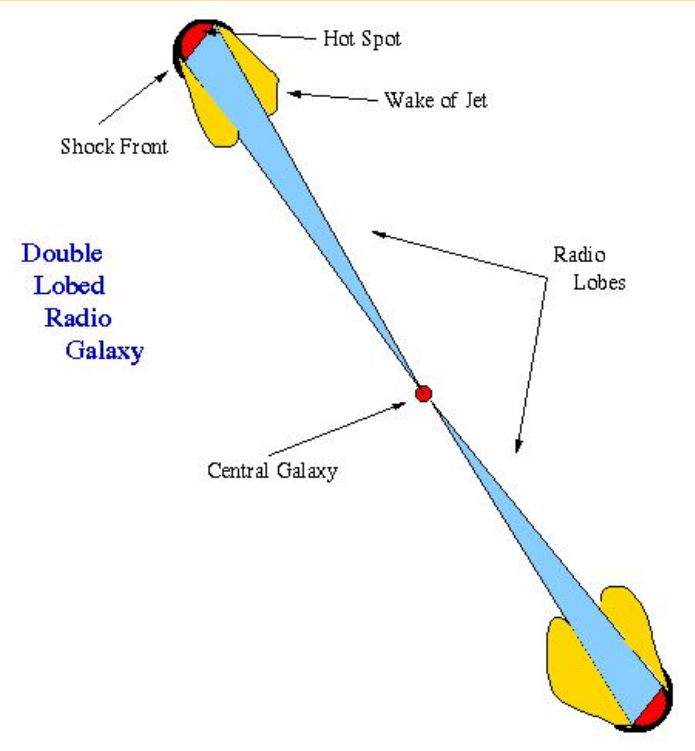

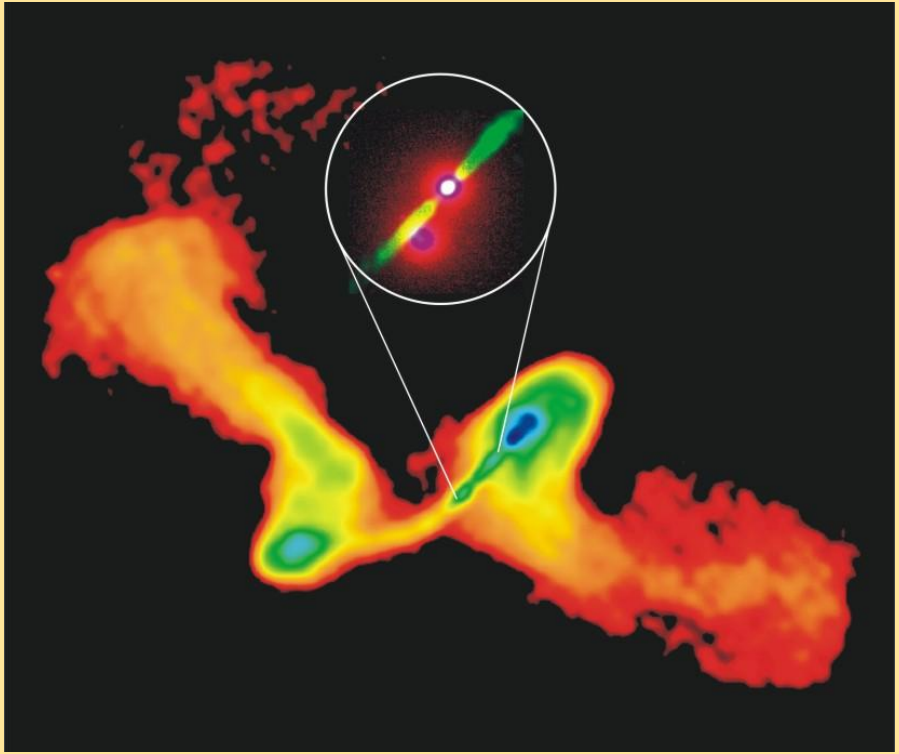

Radio image of the galaxy **NGC 326**,

- Wings were created in an earlier outburst, some tens of Myrs previous to the current renewal of nuclear activity, during which time the ejection axis has precessed.
- Wings are also observed to have a higher spectral index than the active lobes and are highly polarized.
- None of the X-shaped sources shows the broad, optical emission lines associated with quasar activity.
- The host galaxies mostly exhibit high ellipticities and a number have nearby companion galaxies.

Credit: NRAO / AUI, observers Murgia et al.

Koziel-Wierzbowska, D. *et al.* Mon.Not.Roy.Astron.Soc. 422 (2012) 1546-1551

CGCG : 292-057

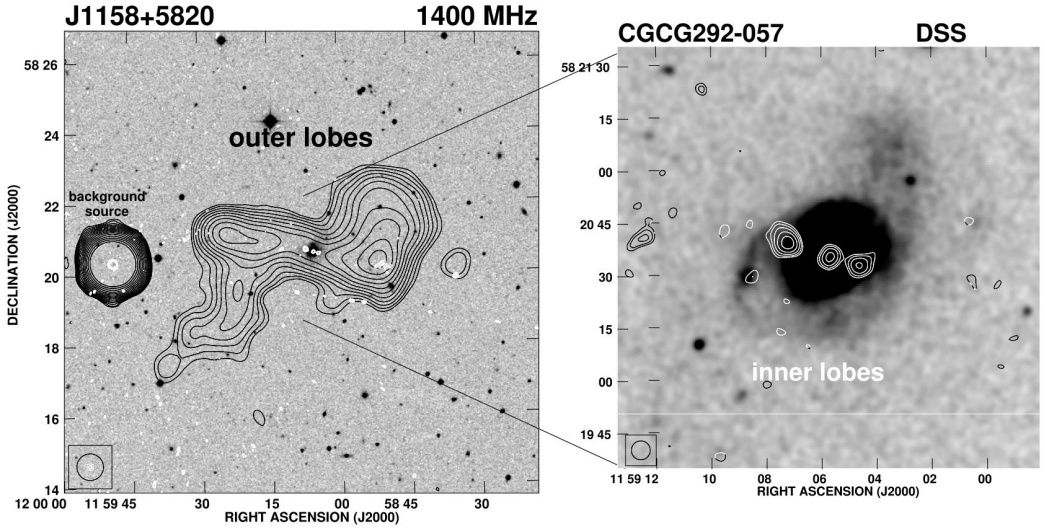

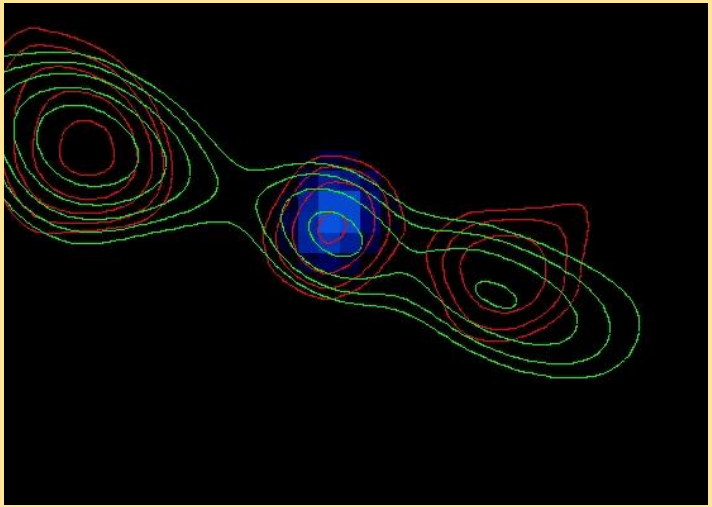

Overlay of 606 MHz & 1400 MHz contours

FIRST (white; beam size ~ 5”). The NVSS map of the target reveals extended radio lobes of the “X-shape morphology”.

we identify this feature with the diffuse phase of the ISM compressed and heated by the expanding jets/lobes.

Jamrozy, M., Kozieł-Wierzbowska, D., Zoła, S. et al. J Astrophys Astron (2011) 32: 467

Chandra ACIS-S

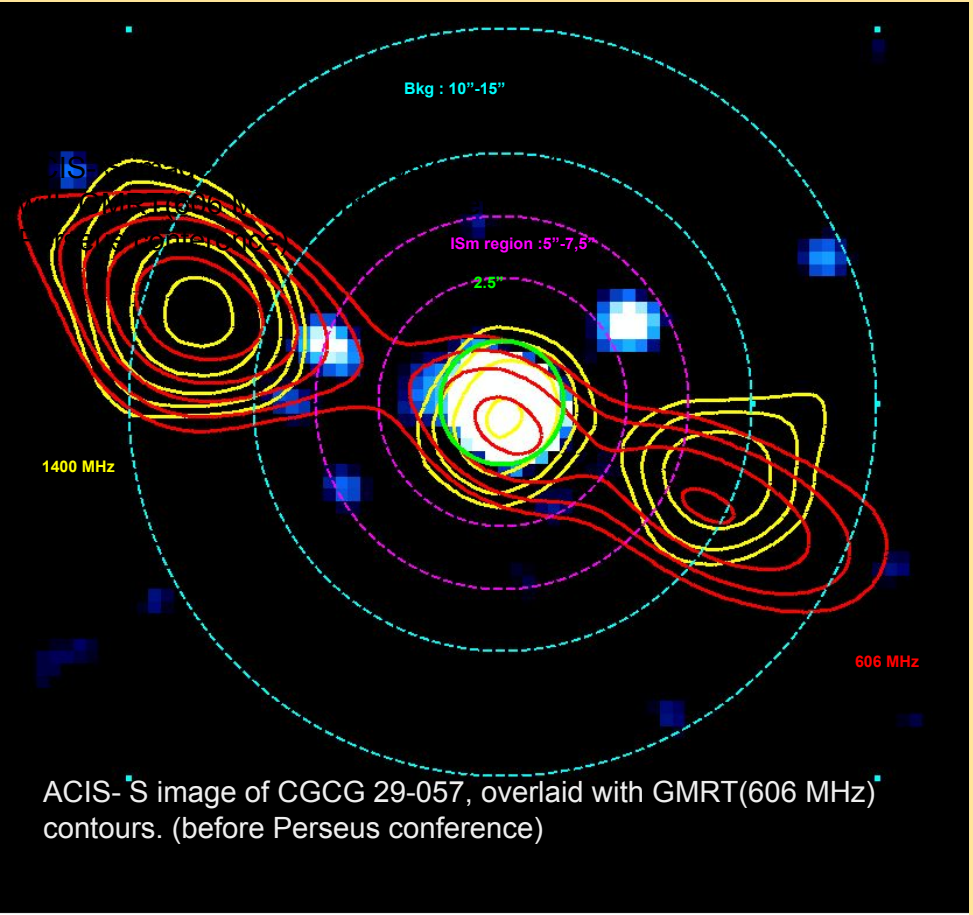

ACIS- S image of CGCG 29-057, overlaid with GMRT(606 MHz) contours. (before Perseus conference)

- **X-ray analysis of the 93 ksec Chandra ACIS−I data for the galaxy CGCG 292−057 (z = 0.054) -> Radio structure with intermittent jet activity.**
- **Performed 100 MARX simulations of the PSF at the position of the active nucleus in CGCG 292−057.**
- **The 2DGaussian fits to the simulated PSFs returned theFWHMs between 1.8 px and 2.1 px, with the corresponding average 3σ source extraction region 1.26 ± 0.04 px.**
- **Excess X-ray emission component is seen around the edges of the innermost parts of the radio structure.**
- **We identify this feature with the diffuse phase of the ISM compressed and heated by the expanding jets/lobes.**

KS - test

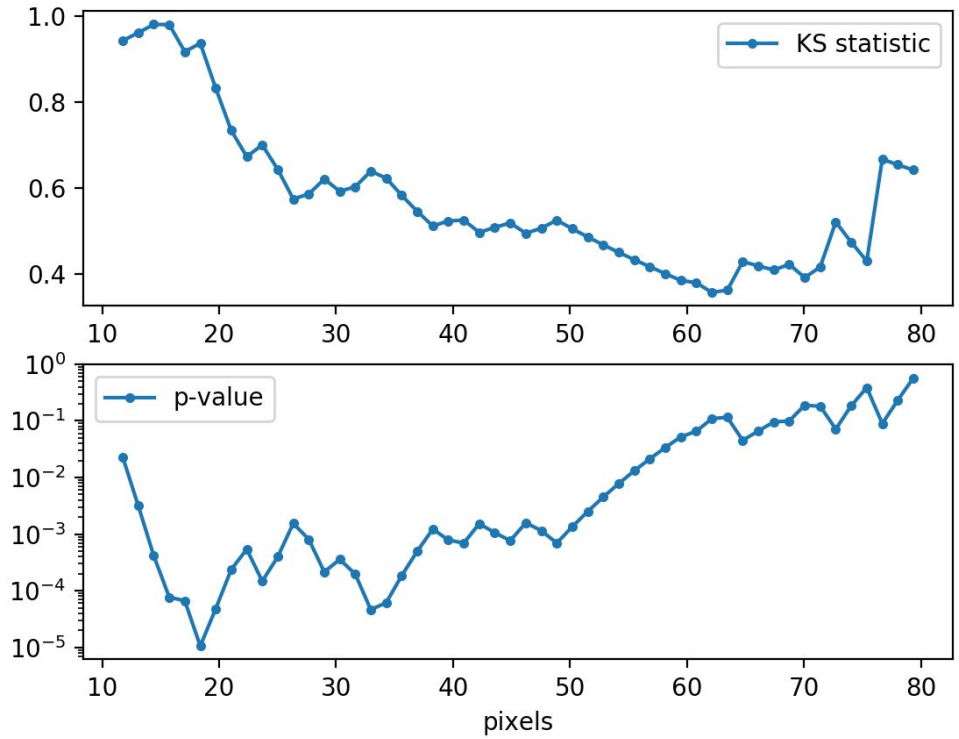

- Positive residuals are seen within the range from about 2.5’’ up to roughly 10’’
- Signalling an additional X-ray emission component located at distances between a few kpc up to about 10 kpc from the core.
- As the p-value reaches the minimum of $\approx 10^{-5}$ at the distance of $\leq$ 20 px from the core.
- In the following spectral analysis of this excess component, we adopt the annular region from 5’’ to 7.5” , and the annular region from 10” to 15” as the constant background

Surface Brightness Profile

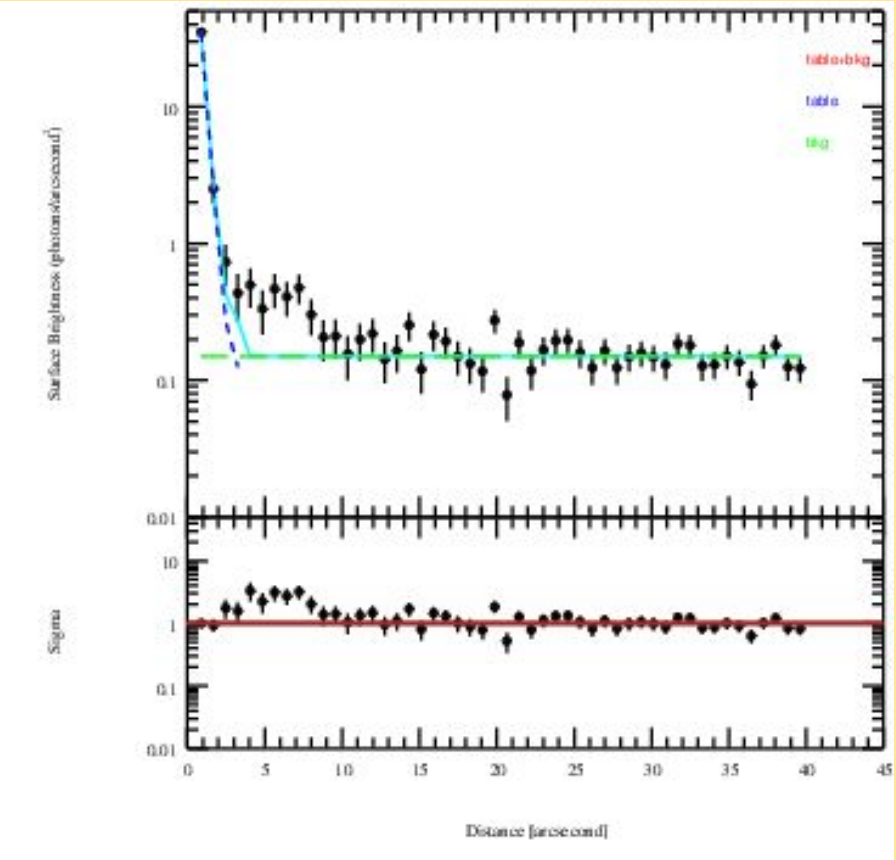

Surface Brightness profile of the source (net counts of concentric stack of annular regions by their respective areas), centred on the CGCG 292−057 nucleus, along with fit including the table model for the PSF (based on the merged simulated PSF images) and a constant background

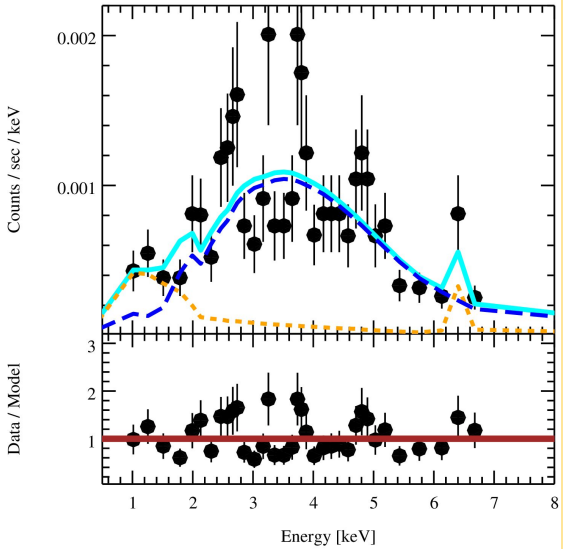

Table 1: Spectral modelling of the CGCG 292−057 nucleus

Model	$N_H^{(1)}$ [$\times 10^{22}$ cm^{-2}]	$N_H^{(2)}$ [$\times 10^{22}$ cm^{-2}]	$kT^{(a)}$ [keV]	$kT^{(b)}$ [keV]	Γ	E_{line} [keV]	EW_{line} [eV]	$Cstat/DOF$
PL	$2.31^{+1.33}_{-1.33}$	—	—	—	$0.61^{+0.53}_{-0.53}$	—	—	726.5/886
PL+G	$2.33^{+0.65}_{-0.65}$	—	—	—	$0.64^{+0.11}_{-0.11}$	$6.75^{+0.07}_{-0.07}$	185 ± 60	772.6/885
bvapec	$4.36^{+0.32}_{-0.28}$	—	> 10	—	—	—	—	732.8/888
bvapec+PL	$0.50^{+0.45}_{-0.45}$	$4.56^{+0.90}_{-0.90}$	$0.71^{+0.22}_{-0.22}$	—	$1.17^{+0.18}_{-0.18}$	—	—	687.75/885
bvapec+bvapec	$0.74^{+0.18}_{-0.18}$	$5.4^{+1.33}_{-1.33}$	> 10	$0.61^{+0.53}_{-0.53}$	—	—	—	688.3/884
Scat. PL+G	$0.076^{+0.024}_{-0.024}$	$6.41^{+1.32}_{-1.32}$	—	—	$1.73^{+0.16}_{-0.16}$	$6.75^{+0.09}_{-0.09}$	241 ± 77	697/883

Data within the range 0.5–7.0 keV; modeled using the C-stat. Fitting optimized with levmar and neldermead methods. Background not subtracted, but modelled. Galactic absorption modeled with phabs assuming $N_{\rm H,Gal} = 0.0143 \times 10^{22}$ cm^{-2}. bvapec metallicities fixed at the solar value. 1σ errors reported.

From the Spectrum of the excess ISM component (5”-7.5”) simultaneously fitted with the bkg (10”-15”)

Results/Discussion

- **Hot diffuse component of the ISM compressed & heated (upto ≤ 1 keV)**
- **$\Gamma \geq 1$ (Inner jets/Compact lobes) ; kT_{ism} = 0.88 keV**
- **Our fits favour the model consisting of a power-law emission scattered by a hot ionized gas giving rise to the 6.7 keV iron line.**
- **power-law photon index $\Gamma > 1$ and the 0.5–7.0 keV L = 5×10^{41} erg/s, consistent with the LINER(**Low-ionization nuclear emission-line region**) classification of the active nucleus in CGCG 292-057.**
- **FeXXV emission due to X-ray reflection on a photoionized circumnuclear matter** ~ **nH** = 6×10^{22} cm^{-2}

- **Scattered power-law emission from hot ionized gas - 6.7 keV**

- **Ionized iron lines have been also detected in the X-ray spectra of the two other compact radio galaxies, namely 0710+439 (Siemiginowska et al.2016), and PMN J1603-4904 (Krauss et al. 2018). (Newly born jets interacting with Multiphase ISM)**

- **Ionized gas could be some dense clouds, engulfed within expanding lobes.**
- **To constrain the nH(ionized), compared with total and neutral (constrained via HI absorption radio features) nH's (Ostorero et al. 2017).**

Bibliography

1. **Kozieł-Wierzbowska, D., et al. 2012, MNRAS, 422, 1546**
2. **Krauss, F., et al. 2018, A&A, 610, 8**
3. **Ostorero, L., et al. 2017, ApJ, 849, 34**
4. **Siemiginowska, A., et al. 2016, ApJ, 823, 57**
5. **Singh, V., et al. 2015, MNRAS, 454, 1556**